A Control Moment Gyro for Dynamic Attitude Control of Small Satellites

Craig Clark
Clyde Space Ltd
West of Scotland Science Park, Glasgow G20 0SP; +44 141 946 4440
craig.clark@clyde-space.com

Dr Kevin Worrall
Clyde Space Ltd
West of Scotland Science Park, Glasgow G20 0SP; +44 141 946 4440
kevin.worrall@clyde-space.com

Emre Yavuzoğlu
Turkish Aerospace Industries, Inc. (TAI)
P.O.Box 18 Kavaklidere, Ankara-Torkiye 06692; (90-312) 811 18 00
eyavuzoglu@tai.com.tr

ABSTRACT

Control Moment Gyroscopes (CMGs) are not often considered for use on small satellites and, as a result few small satellite missions have implemented CMGs as on-board actuators. There are many reasons for this, but mainly this is due the complexity of the mechanical and control system needed to implement an effective CMG, and also because off-the-shelf CMG systems are generally made for the larger satellite market. .CMGs offer many advantages over reaction wheel systems. When used on a small satellite, a CMG based control system can provide the ability to perform very fast slew maneuvers, making CMGs very attractive to high resolution small satellite imaging missions.

The CMG described in this paper incorporates two motors; a Brushless DC Motor (BLDC) and a Stepper Motor. The BLDC provides an efficient means of driving the inertia disk to store the angular momentum, whilst the stepper motor provides precision gimbal control. In order to keep mass and power consumption low, both motors are controlled from a single FPGA. The FPGA runs all associated commutation, speed and position control for both motors and also provides the command and telemetry interface to the rest of the spacecraft. The resulting system is a compact, power efficient design that is ideal for small satellites.

INTRODUCTION

With advances in computer aided design tools and electronics technologies, there are now opportunities to make feasible previously overly challenging concepts. One of these concepts is the use of Control Moment Gyros (CMGs) on small satellites. Up until recently, CMGs have only been used to control the attitude of large spacecraft and space infrastructure such as the International Space Station. However, it is now possible to develop effective, small CMGs for use on small satellites.

Large torque amplification and momentum storage capacity are the two basic properties that make control moment gyroscopes (CMGs) superior when compared to the reaction and momentum wheels. Compared with reaction wheels, CMGs are relatively lightweight and they have a capability to generate higher torque levels per unit kg. This makes CMGs a very promising actuator for future small satellite missions.

This paper describes the development of a single gimbal CMG, designed specifically for small satellite missions. The CMG development was led by Turkish Aerospace Industries with Clyde pace Ltd as a contractor to develop the electronics.

This paper describes the control and interface electronics, demonstrating how the use of relatively new technologies to space, such as FPGAs, can enable more control to be performed locally, without incurring the mass and volume penalties which would normally preclude these control techniques being used on small satellites.

AN INTRODUCTION TO CONTROL MOMENT GYROS

Control moment gyroscopes are momentum exchange devices that rely on the gyroscopic moments to generate torque which is necessary for spacecraft attitude control.

The method of delivery of torque into the spacecraft is achieved by changing the orientation of a spinning disk, which in turn changes the orientation of the disk's angular momentum. Depending on the speed and inertia of the disk, the change in orientation of the disk's angular momentum can represent significant torque levels being exerted on the spacecraft. The beauty of this is that the torques are generated with the need for very little electrical power, unlike reaction wheels where the torque generated is directly proportional to the current supplied to the motor.

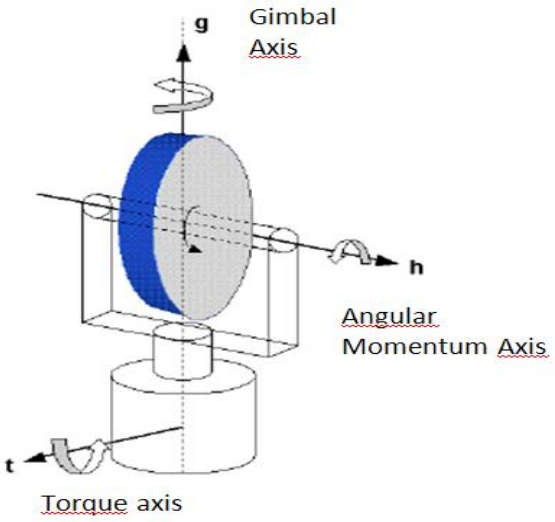

Figure 1 Conceptual schematic of CMG

Just like reaction or momentum wheels, the actuators are also configured as a cluster of four units, providing torque generation capability in all three spacecraft axes as well as adding redundancy. However, the CMG clusters become singular at certain gimbal angle configurations. When singularity occurs, the cluster cannot generate torque in a particular direction. Effective steering logics are developed in the literature to solve singularity problem [1].

The torque production capability of a CMG is directly proportional to the angular momentum of the wheel, while the torque produced with a reaction wheel is only proportional to the inertia of the of the rotors. Thus, it is possible to reduce the weight of a CMG by simply spinning it at higher speeds. Currently, rotor speeds over 15,000 rpm are feasible for space applications. With magnetic bearings, high-speed driver electronics, and much higher-grade (i.e., ISO 1940/1, G 0.4 or better) rotor balancing capabilities, it will be possible to attain much higher spin speeds in the future. The resulting weight savings make them very attractive especially for small satellites.

Another new idea for CMG's design is to have limited gimbal angle travels. With this design, weight of the CMG can further be reduced by eliminating the use of slip rings.

Mainly, there are three design drivers for a CMG system: The spin rate of the rotor, the lubrication at the bearing and the slip ring mechanism used to pass the electrical signals from the rotor to the non-rotating parts. Another issue is related to the steering algorithms used for the CMG cluster. That is, at particular configurations these systems may become singular and cannot generate the necessary torque in a particular direction. A recently developed steering algorithm not only eliminated the impact of singular configurations on satellite attitude control, it has also provided a mean to steer the CMG gimbals toward desirable configuration, while realizing desired maneuver torques [1].

A Comparative Design Study Example

In reference [3], actuator sizing is carried out to meet the ADCS requirements for a conceptual small satellite. Two different CMG designs with different nominal flywheel speeds and RW comparison is provided. Here only the results are provided to demonstrate mass savings for the same torque production capability of different actuators.

Table 1: Reaction Wheel (RW) design results with estimated weight

Parameter	RW
Max. Wheel Speed [RPM]	5000
Max Torque [Nm]	0.2
Angular Momentum Capacity [N m s]	5.2
Flywheel Mass [kg]	1.5
Reaction Wheel Mass [kg]	4

Table 2: Parameters of two CMG designs satisfying the requirements

Parameter	RW	RW
Operating Speed [RPM]	15,000	30,000
Max Gimbal Speed [rad / s]	0.2	0.2
Max Torque [N m]	0.64	0.64
Angular Momentum Capacity [N m s]	3,18	3.18

Flywheel Mass [kg]	0.64	0.3
Total CMG Mass [kg]	3.0	2.1

The table below demonstrates the potential of CMGs compared to RWs:

Table 3: CMG-RW Comparison Table [4]

Parameter	CMG Microsat	Standard Microsat	Minisat
Satellite mass (kg)	50	50	350
Actuator number and type	4 CMGs	4 RWs	4 RWs
Cluster mass (kg)	~1	4	12.8
Power consumption per actuator (Watt)	0.75-4	0.8-3.5	3.3-14
Voltage (V)	5-12	12-16	24-32
Max. Angular Momentum (Nms)	1.1	0.36	4.2
Maximum Torque Production (mNm)	52.5	20	40
Slew Rate Average Speed (°/s)	3	1.85	0.65
Target Satellite MoI (kg-m2)	[2.5, 2.5, 2.5]	[2.5, 2.5, 2.5]	[40, 40, 40]

Summary of advantages of CMGs compared to RWs:

- Agility: Torque amplification property of CMGs makes them ideal selection for demanding missions with stereoscopic imaging, target tracking with high control accuracy, tactical imaging of the target area, formation flying objectives. (Slew rates higher than 3 °/s could be achieved. With RWs 0.1-1°/s can be achieved.)
- With their higher momentum capacities (constant spinning speeds), satellites become more stable platforms.
- Power, mass, volume advantageous compared to alternative actuators as seen in Table 3.

CMG CONTROL ELECTRONICS DESIGN

The Control Moment Gyro developed under this activity incorporates a Brushless DC Motor (BLDC), used for momentum generation, and a Stepper Motor with gearing for the gimbal control system. The control electronics for the motors had strict mass and volume constraints so as to meet the restrictions typical of a small satellite.

Figure 3 shows a simplified block diagram of the control electronics configuration. This figure shows all of the top level units that constitute the control electronics. The main inputs and outputs to the electronics are as follows; the power for the electronics and the motors, the communication bus, the motor control signals for both motors and the feedback signals for both motors.

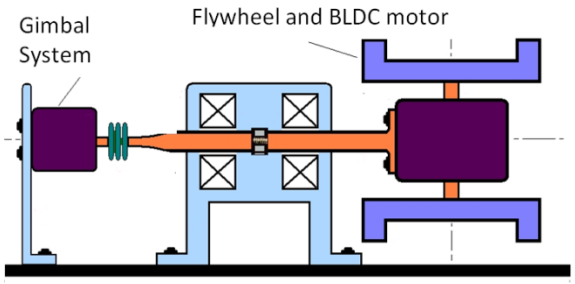

Figure 2 CMG mechanical configuration

The Power Filtering and Conditioning part of the system take the unregulated 28V satellite power bus and regulates it to provide the voltage levels required for the low level control electronics. The input filter must not only suppress noise from the regulators, but also ensure that the noise from the motors is sufficiently to meet the MIL-STD-461F noise requirement.

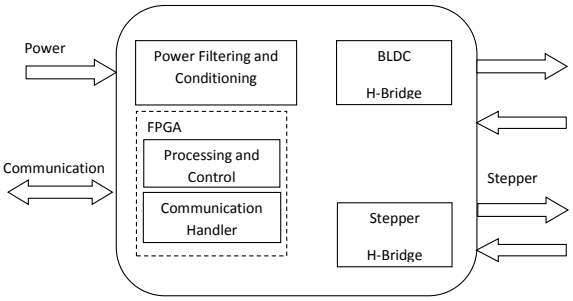

Figure 3 Top Level Block Diagram of the electronics unit

An FPGA provides the required processing, primarily the control and commutation of both motors simultaneously. The FPGA also provides the communications interface to the spacecraft serial data bus. The H-Bridge/3-Phase motor drive stages provide the power interface to the motors.

Due to the units being requirement for use on a Low Earth orbiting small satellite, the radiation requirement was for a minimum of 10krads tolerant.

Figure 4 Motor control, power and filter enclosure.

In order to fit within the volume constraints (163mm x 105mm x 50mm), the functions of the controller has to be split over two printed circuit boards, that were then mounted in 'clam-shell' configuration. The Analogue Board contains the power stage and motor drive electronics and the Digital Board contains the FPGA and control electronics. Figure 6 and Figure 7 show pictures of the engineering models of each board. As can clearly be seen, there are large filter inductors and baluns for the motor power supply on the analogue board; there are also dc-dc converter modules.

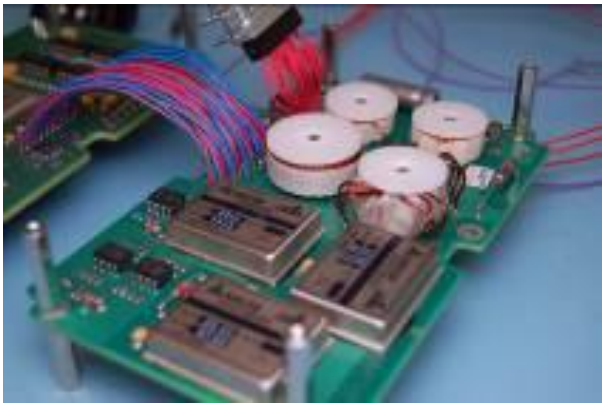

Figure 5 Engineering Model of the Power Board

The FPGA is an 1148 pin BGA from Xilinix and auxiliary electronics can clearly be seen in the Digital Board image, as can the connections between the two boards.

Care also had to be taken to stay within the tight mass constraints; the final mass of the unit was found to be 820g, mostly due to the aluminum housing and large magnetic components.

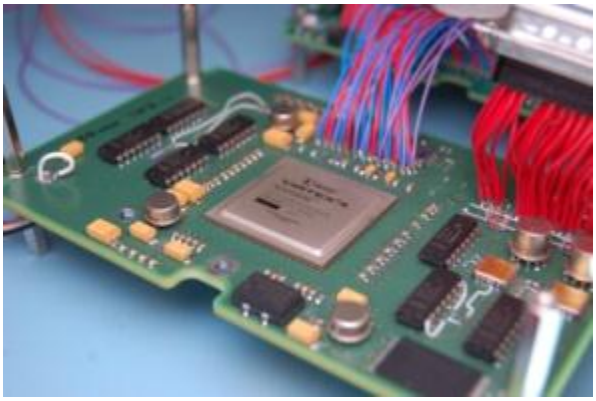

Figure 6 Engineering Model of the FPGA board

Each of the main functions of the control electronics are described in the following sections.

Power Filtering and Conditioning

The control electronics require a number of different voltage levels, as is typical of FPGA designs. Figure 7 provides a block diagram of the power stage. As can be seen the power stage is separated over both an analogue board and a digital board. This approach was taken to ensure a clean split between the low level voltages of the digital parts of the system and the high level voltages of the drive stages and filters. The voltages generated on the digital board are used only on the digital allowing this separation to be achieved. Each stage of the block diagram will be discussed in the next section.

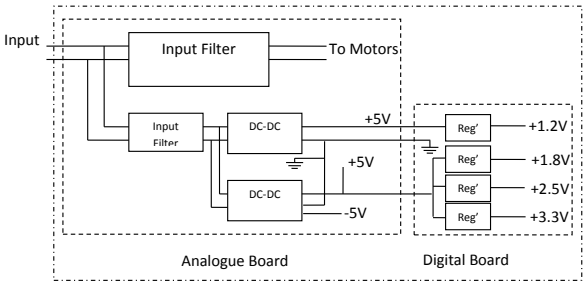

Figure 7 Block Diagram of the Power Stage

Input Filters

The first input filter is designed to ensure that any motor noise generated is not transferred onto the satellite power bus and to provide EMC. The BLDC and Stepper motor driver control circuits are supplied directly from the satellite power bus via this filter, which is a three-stage low-pass filter that provides both differential and common mode filtering across the full frequency spectrum relevant to the design.

In addition to this filter each motor drive has a high performance ceramic decoupling capacitor placed close

to the H-Bridge. Filtering is applied not only to the power lines, but also to the data lines; this because we are concerned both with emissions and susceptibility.

The second input filter supplies the digital electronics via Hi-Reliability DC-DC power supplies. These DC-DC converters are off the shelf parts which have an associated input Hi-Reliability EMI Filter.

DC-DC Converters

The DC-DC converters used are off the shelf parts. Two variants were used, one to supply a high current 5Vand a second to supply both a +5V and a -5V.

The devices used supply a 5V and -5V from a wide range of input voltages, 15 to 50V. The supply from the single 5V converter is routed to the digital board. The additionally required voltages for circuitry on this board are regulated locally. This was done to improve the efficiency of the unit and to help reduce the number of board to board connections required.

The first stage of the digital board power stage is the regulator that provides the 1.2V, actual voltage 1.25V; supplying the core logic of the FPGA. Due to the size of the FPGA selected the required current is high. To meet the current demands a high current linear regulator was used. No other items are run from this regulator, ensuring the required power is delivered to the FPGA core voltage lines.

The digital board also regulates the 1.8V, 2.5V and 3.3V lines for local circuitry in a similar fashion but at much lower power levels.

FPGA and Supporting Circuitry

Central to the system control and implementation is the FPGA. The FPGA handles the communication bus, the motor control signals and general housekeeping of the system. As part of the digital side of the system there is also an Analogue to digital converter, RS422 to serial converters, an oscillator and flash memory which stores the code for the FPGA.

The digital aspects of the system can be represented in block diagram form as shown in Figure 8.

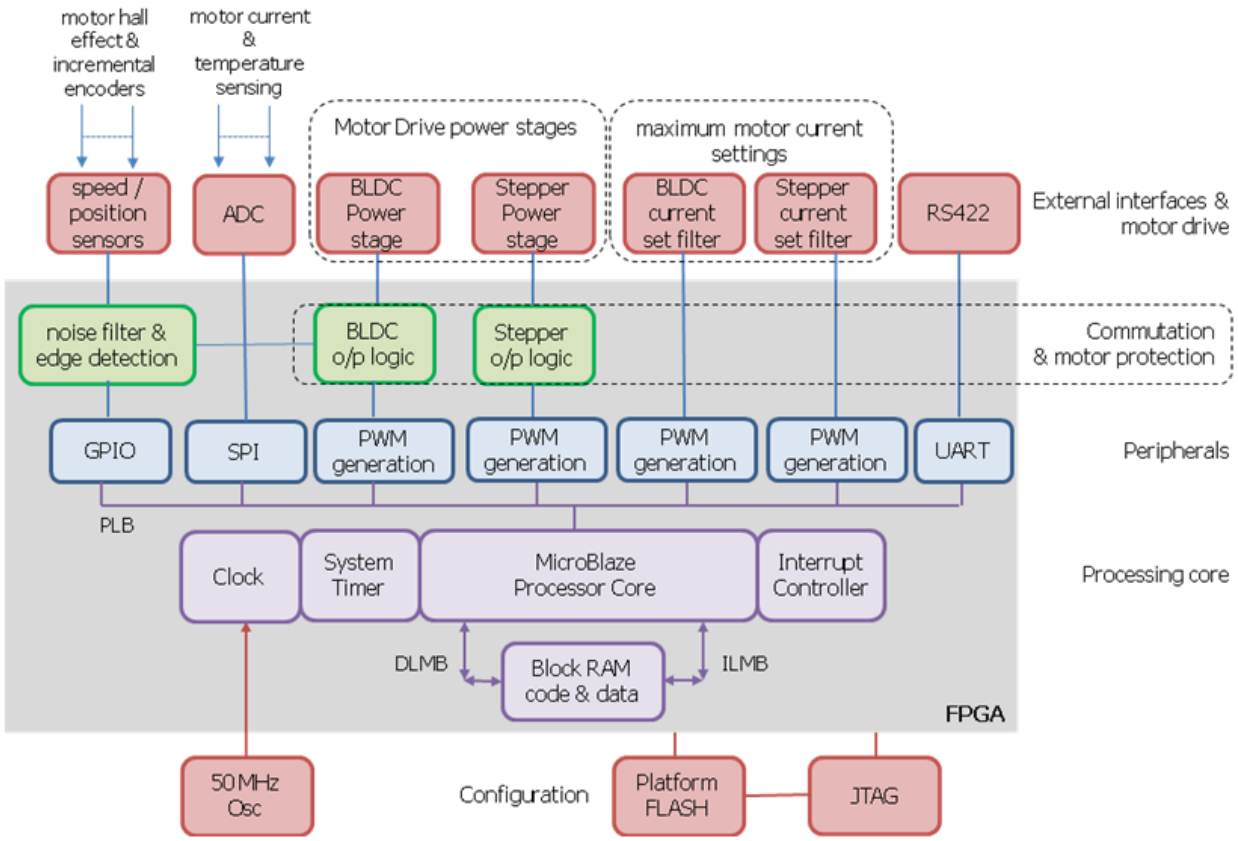

Figure 8 Digital aspects of the System

The FPGA system design comprises software running on an embedded 32 bit processor core coupled with some custom hardware blocks that provide the interface to the external motor drive interfaces. Implementing the motor control algorithms in software allows flexibility in terms of the implementation of the algorithms and also allows for future porting to alternative hardware platforms.

To facilitate any future porting, interfaces between the embedded core and the custom hardware blocks are implemented using simple programmable I/O ports, removing the need to change any interface logic that would be required if a bus based connection scheme had been used.

Speed control of the motors is provided by pulse width modulation of the motor drive under control of the software algorithms, feedback is provided by hall-effect sensors in the BLDC motor and an incremental encoder on the stepper motor.

The system allows the user to monitor and control many aspects of the CMG. The BLDC motor speed can be and the control loop gains can be modified. The telemetry from the BLDC includes the current speed, the current draw and the temperature of the motor. Telecommand and telemetry of the Stepper motor are the same as for the BLDC, but include also conntinuous movement, position control, direction control and position.

Motor Control and drive stages

Figure 9 details a block diagram representation of how the motor control system works.

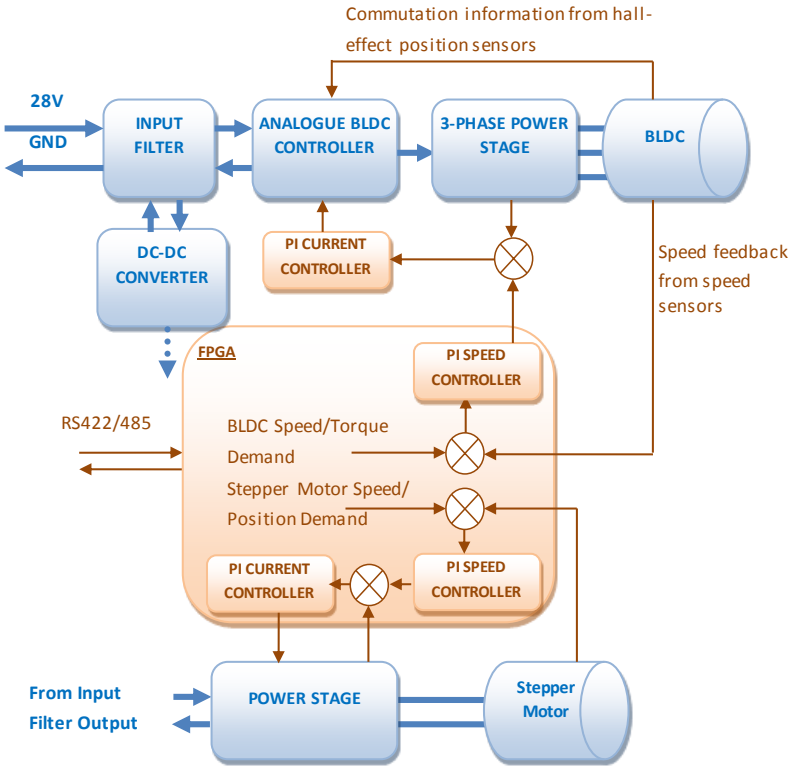

Figure 9 Block diagram representation of the Motor Control

To provide current feedback for current limiting and current telemetry for both motors, there is a current sense circuit for each drive stage. This signal is routed through an ADC to provide the relevant information to the FPGA program.

A PI controller runs on the FPGA to control the speed of the motor. Commutation between the phases of the BLDC motor is provided by a commutation sequence programmed in the FGPA in Verilog. Hall-effect

sensors in the motor provide position feedback of the rotor and these signals feed directly into the FPGA.

The power stage of the BLDC motor drive circuitry is a 3-phase full-bridge configuration. This circuit is capable of switching all three phases of the motor, driving the motor in braking and acceleration mode in either clockwise or anti-clockwise directions.

The drive circuitry used for the stepper motor is two independent H-Bridges, an example of which is shown in Figure 10.

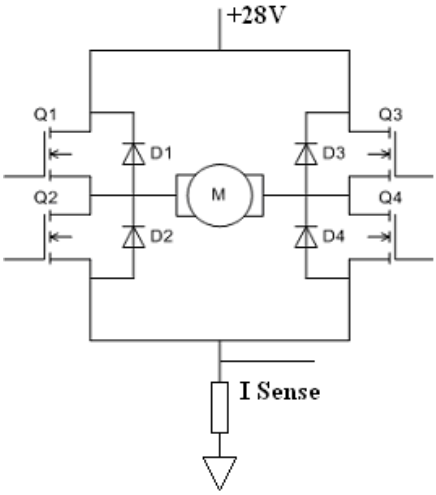

Figure 10 Example standard single H-Bridge

To drive the Stepper Motor the Half Stepping Drive technique is used. Each phase of the stepper motor is driven by a separate H-bridge, allowing for more precise control of its rotation in both clockwise and anti-clockwise direction.

ENVIRONMENTAL TESTING

Being a new development, the system required significant qualification and verification testing. Due to the time constraints on the development project, it was necessary to process and test the electronics separately to begin with using a test rig to ensure that the electronics meet the strict EMC and vibration requirements of the end system.

The first tests to be performed were radiation. All of the electronics used in the design were to a MIL standard, but were not specifically radiation tolerant. A number of components were subject to radiation tests to ensure that they could survive at least until 10krads. In fact, it was proven that the components could survive up to 30krads without significant degradation of performance. These tests included the FPGA.

Figure 11 shows one of the set-ups for EMC testing. At the bottom of the picture there is a simulation of the CMG electro-mechanical hardware. This consists of an identical BLDC with flywheel; this motor is run up to the desired 10,000RPM to demonstrate the operational speed range. The inertia of the flywheel is approximately $4.8 \times 10^{-4} kgm^2$.

In addition, there is an identical stepper motor to the expected flight unit, plus a gearing system. The disk wrapped with blue tape is a brake, providing an equivalent load to the angular momentum of a spinning disk of the BDLC – this is equivalent to an inertial load (before the gearbox) of$2.6 \times 10^{-3} kgm^2$. This test set-up provided a means to easily test the CMG electronics throughout the development and test phases.

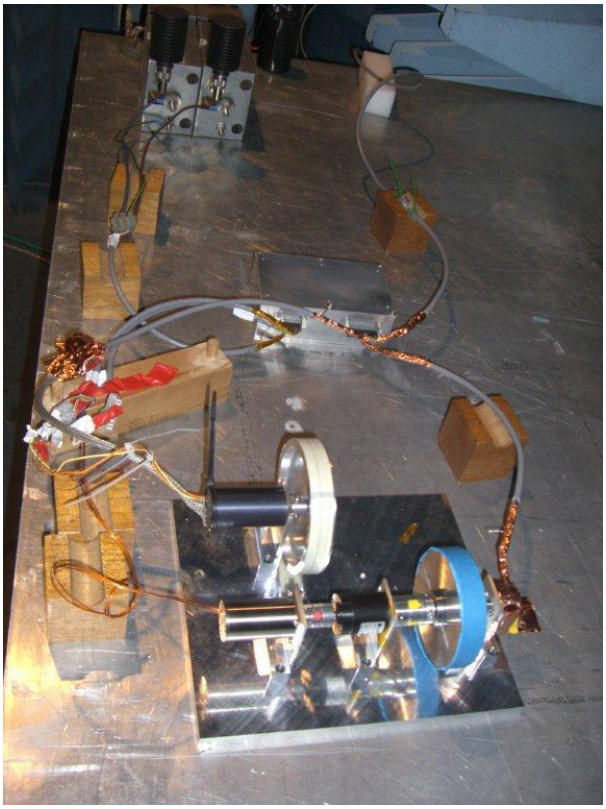

Figure 11 EMC Test set-up

EMC testing to MIL-STD-461E consisted of an extensive range of conducted and radiated susceptibility and emissions. Figure 12 shows the unit being subjected to a radiated susceptibility test.

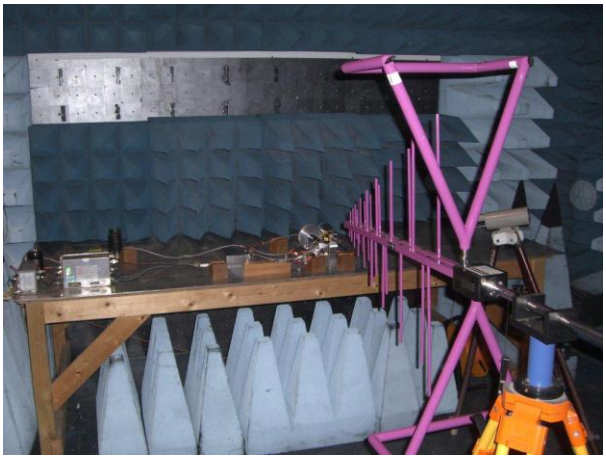

Figure 12 Radiated Susceptibility testing of the unit

Anyone who has had the pleasure of performing EMC tests will understand that we were delighted to pass all tests with only some minor adjustments to the input filters.

With EMC tests complete, the next test was vibration. We produced a Qualification Model (QM) and seven Flight Models (FMs) of the electronics. The QM was subjected to relatively high sinusoidal and random vibration levels (16.8g RMS), and shock levels. The QM passed all tests. The picture below shows the QM on the vibration table. The QM unit was then subject to further qualification tests in a Thermal Vacuum Chamber (-40˚C to +70˚C).

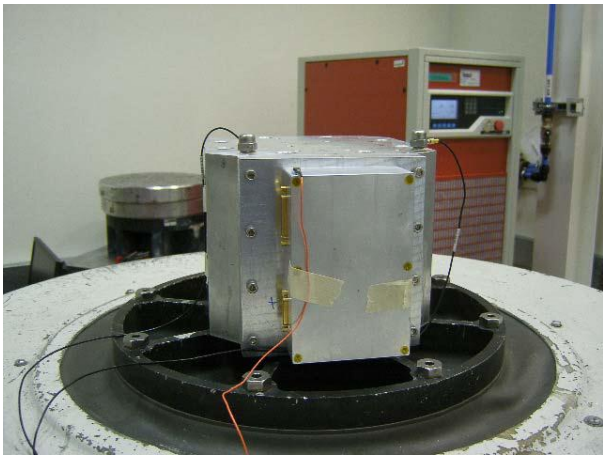

Figure 13 Qualification model on vibration table.

Following the completion of the Qualification tests, the Flight model units were then subject to acceptance level testing. Figure 14 shows three of the FMs prepared and about to be sealed in the thermal vacuum chamber.

Figure 14 Flight Models prepared for thermal vacuum testing.

With all environmental testing completed, the electronics were shipped off to TAI for integration with the qualification and flight model CMG electro-mechanics.

Due to the sensitive commercial nature of the CMG mechanical configuration, it is not possible to show pictures of the finished unit. The complete unit was subject to the same qualification and acceptance tests as for the electronics, and all tests were passed satisfactorily. There are no seven small satellite CMG units sitting ready for use on future small satellites.

CONCLUSION

As a direct result of advances in technology and control techniques, it is now possible to consider CMGs a an alternative to reaction wheels for small satellite missions. This project has shown that high performance control electronics can be produced to meet the tight mass and volume constraints demanded by small satellite missions. Also, advances in motors, bearings and lubricants have enabled more robust mechanical configurations to be adopted to meet and survive the challenging mechanical environment typically experienced by small satellites. We now wait with anticipation for feedback from the in-flight performance of the CMG based attitude control system for small satellites.

Acknowledgments

The authors acknowledge the exceptional effort of the design and production teams from TAI and Clyde Space in order to complete the development and production project within what was a very tight schedule.

References

1. Tekinalp, O., Yavuzoglu, E., "A new steering law for redundant control moment gyroscope clusters," Aerospace Science and Technology, Vol. 9, No. 7, pp. 626-634, October, 2005.
2. Tekinalp, O., Yavuzoglu, E., Solakoglu, E., " Conceptual Design of Cheap, Modular, Light Weight Control Moment Gyroscopes for Small Satellites," NATO RTO Emerging and Future Technologies, Turkey, 2010.
3. Tekinalp, O., Yavuzoglu, E., Solakoglu, E., Altay, A., "Control Moment Gyros for Attitude Control and Energy Storage in Small Satellite Missions," NATO RTO Emerging and Future Technologies, Romania, 2006.
4. Lappas V. J., A Control Moment Gyro Based Attitude Control System For Agile Satellites, PhD Thesis, University of Surrey, Guildford, Surrey, United Kingdom, October 2002.